AIP | Physics of Plasmas

Envelope-kinetic analysis of the electron kinetic effects on Raman backscatter and Raman backward laser amplification

Min Sup Hur, Seung Hoon Yoo, and Hyyong Suk

Citation: Physics of Plasmas (1994-present) **14**, 033104 (2007); doi: 10.1063/1.2646493

View online: http://dx.doi.org/10.1063/1.2646493

View Table of Contents: http://scitation.aip.org/content/aip/journal/pop/14/3?ver=pdfcov

Published by the AIP Publishing

Envelope-kinetic analysis of the electron kinetic effects on Raman backscatter and Raman backward laser amplification

Min Sup Hur
Center for Advanced Accelerators, Korea Electrotechnology Research Institute, Changwon, Kyongnam 641-120, Korea

Seung Hoon Yoo
Center for Advanced Accelerators, Korea Electrotechnology Research Institute, Changwon, Kyongnam 641-120, Korea and Department of Physics, Chung-Ang University, Seoul 156-756, Korea

Hyyong Suk[a)]
Center for Advanced Accelerators, Korea Electrotechnology Research Institute, Changwon, Kyongnam 641-120, Korea

(Received 17 November 2006; accepted 19 January 2007; published online 8 March 2007)

The electron kinetic effects on Raman backscattering and Raman backward laser amplification were analyzed. The analysis is based on the envelope-kinetic equations of a plasma wave, which are composed of the conventional envelope equation of a fluid plasma and the kinetic term. One major goal of this paper is to close the envelope-kinetic model by analyzing the kinetic term, which was not fully covered in the previous work [M. S. Hur *et al.*, Phys. Rev. Lett. **95**, 115003 (2005)]. It was found that the closed envelope-kinetic equation in the nontrapping regime takes the same form as the envelope equation of the fluid plasma used in the three-wave model. For the closure in the trapping-dominant regime, the test particle technique is employed to calculate the kinetic term. Results from the full kinetic and test particle simulations agree well with each other, while the latter has a great advantage in computation speed. The frequency shift and resonance breaking by the trapped particles are discussed with the help of a new diagnostic inserted in the full kinetic averaged particle-in-cell code. © *2007 American Institute of Physics*. [DOI: 10.1063/1.2646493]

I. INTRODUCTION

The Raman backward scattering (RBS) of a laser pulse in a plasma has been an interesting issue due to its wide applications as well as rich physics in itself. For instance, the reflection of lasers in a plasma by RBS and the stimulated Brillouin scattering (SBS) has been studied intensively in connection with inertial confinement fusion research.[1–6] One of the major issues in those works was the kinetic effect on the saturation or enhanced Raman reflectivity. It was found there by kinetic simulations and analysis that the trapped electrons reduce the linear Landau damping in a high temperature plasma. The result was the enhanced RBS over the prediction from the fluid model.[5] It was also found that RBS is saturated by trapping-induced secular phase shift between the Langmuir wave and the lasers. Another important physics was pointed out by Brunner *et al.*, where they found that the Langmuir wave breakup induced by the trapped particle instability can lead to the saturation and periodic bursting of the RBS.[6]

The importance of the similar kinetic effects[7] could also be found in the Raman backward laser amplifier (RBA).[8] RBA is a novel scheme of laser amplification using Raman backscattering in a plasma, which was proposed to overcome the material damage threshold of gratings in the conventional chirped-pulse-amplification (CPA).[9] The major advantage of the RBA is that it does not require stretch and recompression of the laser pulse since the critical power the plasma can bear ($P_{cr} \simeq 17\omega^2/\omega_p^2$ GW) (Ref. 10) is much higher than those of other gaseous or solid materials. The idea of RBA has been investigated by theories and simulations[8,11–13] and it also has been realized successfully in many experiments.[14–16] As in the inertial confinement fusion system mentioned above, RBA is also influenced considerably by the kinetic effects such as the Langmuir wave breaking and particle trapping. From the full kinetic simulations, it was found that the pump depletion can be significantly reduced[7,11,12] when the RBA is operated over the Langmuir wave breaking limit. Recently it was shown from detailed study of the electron phase space that not a complete wave breaking but just a small fraction of trapped particles inside the unbroken plasma wave could lead to a much earlier RBS saturation.[7] The most important feature of that work is the derivation of the envelope-kinetic equation for a plasma wave, which is composed of the usual envelope equation used in the fluid three-wave model and a new kinetic term.

The analysis of the trapping effects in the previous work,[7] however, was not fully closed in the sense that the kinetic term was measured from independent simulations, not from the model itself. In this paper we present the test particle method to complete the envelope-kinetic model of the plasma wave. This method is based on using a small number of test particles to calculate the kinetic contribution. With the kinetic term computed at a given time step from the test particles, the electric field is upgraded to the next time step by solving the envelope-kinetic plasma equation. Then

[a)]Electronic mail: hysuk@keri.re.kr

the test particle motion is determined by the electric field and the ponderomotive force of the lasers. It will be shown that the test particle simulations agree well with the full kinetic simulations. In addition to closing the model in the trapping regime, we present a detailed analysis of the kinetic term in the nontrapping regime. The envelope-kinetic plasma equation is generalized to higher harmonic envelopes. The thermal shift of the Langmuir wave frequency and the linear Landau damping are derived from the linear analysis of the kinetic term. Its third-order expansion is found to be cancelled by the harmonic of the same order. The resultant closed form of the envelope-kinetic equation in the nontrapping regime is the same as what is used in the conventional three-wave fluid model. This result also implies that there should be no nonrelativistic frequency shift in the plasma wave frequency at least up to the third order when the particle trapping is not involved.

This paper is organized as follows: In Sec. II a general envelope-kinetic plasma equation is derived. It is followed by analysis of the kinetic term in the nontrapping regime in Sec. III. In Sec. IV the effects of the trapped particles on the RBA are investigated. We also present the test particle method to describe the kinetic term. Finally the summary is given in Sec. V.

II. ENVELOPE-KINETIC EQUATIONS OF A PLASMA WAVE

Envelope-kinetic equations for lasers are commonly used in free-electron-laser (FEL) simulations. Similar equations were applied to RBS problem first by Shvets *et al.* in Refs. 17 and 18 to study the laser amplification in the superradiant regime. The equations take the following forms:

$$\frac{\partial a_1}{\partial t} + c\frac{\partial a_1}{\partial z} = -i\frac{\omega_p^2}{2\omega_1}a_2\langle e^{+i\phi_j}\rangle,$$
$$\frac{\partial a_2}{\partial t} - c\frac{\partial a_2}{\partial z} = -i\frac{\omega_p^2}{2\omega_2}a_1\langle e^{-i\phi_j}\rangle, \tag{1}$$

where $a_{1,2}$ are the envelopes of the seed and pump lasers respectively, $\omega_{1,2}$ the laser frequencies, ϕ_j is the ponderomotive phase of the jth particle defined by $\phi_j=-(k_2+k_1)z_j-(\omega_2-\omega_1)t$. The position of jth particle, z_j, is a function of time. Note that we are considering the case where the seed laser is propagating to the right and the pump laser in the opposite direction. Equations (1) were combined with the conventional particle-in-cell (PIC) method to produce the averaged particle-in-cell (aPIC) code for the kinetic simulations of RBS and the laser amplification.[13]

In this paper, we derive the envelope-kinetic equation for a nonrelativistic one-dimensional plasma wave. Extending the previous work,[7] the derivation is generalized to higher harmonics of the plasma wave. The starting equations are the Poisson equation and the harmonic expansion of the electric field. When there is a collection of point charges (electrons) as a source term, the Poisson equation takes the following form:

$$\frac{\partial E_z}{\partial z} = -\frac{e}{\epsilon_0}\sum_j \delta(z-z_j), \tag{2}$$

where the Dirac delta function represents the point charge density of each electron located at z_j. The electric field is expanded by harmonics as

$$E_z = \frac{1}{2}\sum_n \hat{E}_n(t)e^{in\phi} + \text{c.c.}, \quad \phi = kz-\omega t, \tag{3}$$

where k and ω are the wave number and frequency of the plasma wave, respectively. The nth harmonic envelope $\hat{E}_n$ can be obtained by inserting Eq. (3) into the Poisson equation (2) and spatially averaging over a plasma wavelength λ weighted by $e^{-in\phi}$. Then

$$\frac{ik}{2}n\hat{E}_n = -\frac{e}{\lambda\epsilon_0}\sum_j e^{-in\phi_j}, \tag{4}$$

where $\phi_j=kz_j-\omega t$ and the index j goes over the particles inside a plasma wavelength, i.e., $k|z_j-z|\leq\pi$. In the derivation of Eq. (4), the averaging operation on the envelope was neglected from the assumption that the envelope $\hat{E}_n$ is a slowly varying function of time and space. A dimensionless variable F_n is defined by the nth envelope normalized by the wavebreaking limit of a cold plasma, $F_n\equiv e\hat{E}_n/mc\omega_p$. Then from Eq. (4)

$$F_n = i\frac{2\omega_p}{nck}\langle e^{-in\phi_j}\rangle, \tag{5}$$

where ω_p is the cold plasma frequency. It is assumed that the wave frequency, which is the same as the driving frequency, is very close to ω_p (almost resonant driving). The angular bracket is defined by $\langle Q_j\rangle=\Sigma_j Q/N_0$, where $N_0=n_p\lambda$ is the initial (unperturbed) number of electrons in a plasma wave bucket in the one-dimensional limit.

To derive the equation of F_n, we start from the first and second time derivatives of $F_n(z,t)$,

$$\frac{\partial F_n}{\partial t} = 2\omega_p\langle\beta_j e^{-in\phi_j}\rangle + in\omega F_n, \tag{6}$$

and

$$\frac{\partial^2 F_n}{\partial t^2} = 2\omega_p\langle\dot{\beta}_j e^{-in\phi_j}\rangle - 2inck\omega_p\langle\beta_j^2 e^{-in\phi_j}\rangle + 2in\omega\omega_p\langle\beta_j e^{-in\phi_j}\rangle + in\omega\frac{\partial F_n}{\partial t}, \tag{7}$$

where $\beta_j=v_j/c$ and $v_j=\mathrm{d}z_j(t)/\mathrm{d}t$ is the jth particle velocity. The acceleration $\dot{\beta}_j$ can be obtained from the equation of motion of a single electron

$$\dot{\beta}_j = -\frac{e}{mc}E(z_j,t) + P(z_j,t), \tag{8}$$

where $P(z_j,t)$ is any kind of a driving force. Later in Sec. IV where RBS and the RBA are addressed, $P(z_j,t)$ will be replaced by the ponderomotive force of the two counterpropagating lasers. From Eqs. (7) and (8) and eliminating $\langle\beta_j e^{-in\phi_j}\rangle$ using Eq. (6) yields

$$\frac{\partial^2 F_n}{\partial t^2} = -\frac{2e\omega_p}{mc}\langle E(z_j,t)e^{-in\phi_j}\rangle + 2\omega_p\langle P(z_j,t)e^{-in\phi_j}\rangle - 2inck\omega_p\langle\beta_j^2 e^{-in\phi_j}\rangle + n^2\omega^2 F_n + 2in\omega\frac{\partial F_n}{\partial t}. \quad (9)$$

The averaged electric field term in Eq. (9) is, from Eqs. (3) and (5),

$$\langle E(z_j,t)e^{-in\phi_j}\rangle = -i\frac{mc^2k}{4e}\sum_{n'=1}^{n-1}(n-n')F_{n'}F_{n-n'} + \frac{mc\omega_p}{2e}F_n - i\frac{mc^2k}{4e}n\sum_{n'=1}^{\infty}F_{n+n'}F_{n'}^*. \quad (10)$$

From Eqs. (9) and (10), the equation of F_n becomes

$$\frac{\partial F_n}{\partial t} + \frac{i}{2n\omega}(\omega_p^2 F_n - n^2\omega^2 F_n) - \frac{ck\omega_p}{\omega}\langle\beta_j^2 e^{-in\phi_j}\rangle + \frac{i}{2n\omega}\frac{\partial^2 F_n}{\partial t^2} = -\frac{ck\omega_p}{4n\omega}\sum_{n'=1}^{n-1}(n-n')F_{n'}F_{n-n'} - \frac{ck\omega_p}{4\omega}\sum_{n'=1}^{\infty}F_{n+n'}F_{n'}^* + i\frac{\omega_p}{n\omega}\langle P(z_j,t)e^{-in\phi_j}\rangle. \quad (11)$$

The second term in the left-hand side (LHS) of Eq. (11) describes the detuning between the driving frequency ω (and its harmonics) and the characteristic frequency ω_p of an undriven plasma wave. The third one in the LHS is the kinetic term which reflects the kinetic features such as thermal effect, Landau damping, and particle trapping. The second time derivatives are generally neglected by assuming a slowly varying envelope.

We pursue up to $n=2$ of Eq. (11). For $n=1$ Eq. (11) becomes

$$\frac{\partial F_1}{\partial t} + i\delta\omega F_1 - \frac{ck\omega_p}{\omega}\langle\beta_j^2 e^{-i\phi_j}\rangle = -\frac{ck\omega_p}{4\omega}F_2F_1^* + i\frac{\omega_p}{\omega}\langle P(z_j,t)e^{-i\phi_j}\rangle, \quad (12)$$

where $\delta\omega=\omega_p-\omega$. We neglected $\delta\omega^2$ assuming a very small mismatch between the driving and the plasma frequency. We keep the third harmonic because the leading order of the kinetic term for a cold plasma is the third in the nontrapping regime. If the driving force $P(z_j,t)$ is replaced by the ponderomotive beat wave by two counterpropagating lasers, Eq. (12) becomes the same as the result in Ref. 7. Similarly for $n=2$,

$$\frac{\partial F_2}{\partial t} + \frac{i(\omega_p^2-4\omega^2)}{4\omega}F_2 - \frac{ck\omega_p}{\omega}\langle\beta_j^2 e^{-2i\phi_j}\rangle = -\frac{ck\omega_p}{8\omega}F_1^2 - \frac{ck\omega_p}{4\omega}F_3F_1^*. \quad (13)$$

The external driving $P(z_j,t)$ is omitted from Eq. (13) assuming the case where the high harmonic component in the driving force is only slowly varying. Note that no assumption on the plasma temperature was made in obtaining Eqs. (12) and (13). Thus these envelope-kinetic equations are valid for general temperature plasmas including Raman backward laser amplification and inertial confinement fusion plasmas. In the following sections, we focus more on the Raman backward amplification, where the thermal velocity of the plasma is comparable to or less than the phase velocity of the plasma wave.

III. ANALYSIS OF THE KINETIC TERMS IN THE NONTRAPPING REGIME

It is useful to have some rough estimations of the kinetic term before doing any rigorous analysis. The velocity can be expanded as $\beta=\beta_t+\beta_1+\beta_2+\cdots$, where β_t represents the thermal velocity (or a beam component, which is not considered in this paper). Other terms represent the oscillations by the electric field of the plasma wave and by the ponderomotive force of the lasers. Note that the order of β_t does not always need to be larger than those of β_n's. The kinetic term for $n=1$ is estimated by $\langle\beta_j^2 e^{-i\phi_j}\rangle \sim (\langle\beta_{t,j}^2\rangle + 2\langle\beta_{t,j}\beta_{1,j}\rangle + \langle\beta_{1,j}^2\rangle + \cdots)\langle e^{-i\phi_j}\rangle \sim (\overline{\beta_t^2}+|F_1|^2)F_1$, where we assumed $\langle\beta_t\beta_1\rangle \sim \bar{\beta}_t\bar{\beta}_1 \sim 0$ for a symmetric initial velocity distribution and used $\beta_1 \sim F_1$. The estimation combined with $i\delta\omega F_1$ in Eq. (12) gives the total detuning $\delta\omega_{\text{total}} \sim (\omega_p + \overline{\beta_t^2} + |F_1|^2) - \omega = \Omega_p - \omega$. The contribution of $\overline{\beta_t^2}$ to the modified plasma frequency Ω_p corresponds to the thermal shift in the Langmuir wave frequency, which is described by $\omega_L \simeq \omega_p(1 + 1.5k^2\overline{v_t^2}/\omega_p^2)$. The second-order frequency modification from $|F_1|^2$ seems like a nonlinear shift in the plasma frequency, which was once controversial in the past.[19–22] The conclusion was that there is no nonlinear frequency change other than the relativistic effect. Our formulation is also consistent with this conclusion; it will be shown later that $|F_1|^2$ in Ω_p is cancelled by F_2 term in the RHS of Eq. (12).

In this section, the exact form of the thermal shift $(1.5k^2\overline{v_t^2}/\omega_p^2)$ is derived from the kinetic term. To do this, we use the velocity distribution function and the Vlasov equation. During the derivation, the linear Landau damping coefficient is also obtained. The second harmonic F_2 is represented in terms of F_1, whose result is the same as what can be obtained from the fluid equations. The third-order terms are also investigated, and they are shown to be cancelled by each other.

A. Thermal Langmuir frequency and Landau damping

For the particle distribution function $g(z,\beta,t)$, the kinetic term can be represented by

$$-\frac{ck\omega_p}{\omega}\langle\beta_j^2 e^{-in\phi_j}\rangle = -\frac{ck\omega_p}{\omega\lambda}\int_\lambda dz\int d\beta g(z,\beta,t)\beta^2 e^{-in\phi}, \quad (14)$$

where λ is the plasma wavelength. The velocity distribution $g(z,\beta,t)$ is assumed to be expanded as

$$g(z,\beta,t) = g_0(\beta) + \tfrac{1}{2}[\hat{g}_1(\beta)e^{i\phi} + \text{c.c.}] + \tfrac{1}{2}[\hat{g}_2(\beta)e^{2i\phi} + \text{c.c.}] + O(3). \quad (15)$$

Note that the amplitudes g_0 and $\hat{g}_{1,2}$ do not have any depen-

dence on z, since the integration is performed over one plasma wavelength on which the change in the plasma wave envelope can be neglected by the slowly varying assumption. From $\int_\lambda e^{in\phi}dz=0$ for $n\neq 0$, the first and second kinetic terms are represented by

$$-\frac{ck\omega_p}{\omega}\langle\beta_j^2 e^{-i\phi_j}\rangle=-\frac{ck\omega_p}{2\omega}\int \hat{g}_1(\beta)\beta^2 d\beta \tag{16}$$

and

$$-\frac{ck\omega_p}{\omega}\langle\beta_j^2 e^{-2i\phi_j}\rangle=-\frac{ck\omega_p}{2\omega}\int \hat{g}_2(\beta)\beta^2 d\beta. \tag{17}$$

The amplitudes $\hat{g}_1$ and $\hat{g}_2$ are determined by the linearized and the second-order Vlasov equations. Then

$$\hat{g}_1=i\omega_p F_1\frac{\partial_\beta g_0}{\omega-ck\beta} \tag{18}$$

and

$$\hat{g}_2=-\frac{\omega_p^2}{4}F_1^2\frac{\partial_\beta^2 g_0}{(\omega-ck\beta)^2}-\frac{ck\omega_p^2}{4}F_1^2\frac{\partial_\beta g_0}{(\omega-ck\beta)^3}+i\frac{\omega_p F_2}{2}\frac{\partial_\beta g_0}{\omega-ck\beta}. \tag{19}$$

Note that the acceleration by the ponderomotive force was not included in Eqs. (18) and (19). This is valid in the Raman regime, where the ponderomotive driving is much smaller than the electrostatic force.

The kinetic term with $n=1$ is calculated from Eqs. (16) and (18). Using the Plemelj formula, we obtain

$$\begin{aligned}-\frac{ck\omega_p}{\omega}\langle\beta_j^2 e^{-i\phi_j}\rangle&=-\frac{ick\omega_p^2F_1}{2\omega}\left(\int d\beta\frac{\beta^2\partial_\beta g_0}{\omega-ck\beta}+\frac{i\pi\omega^2}{c^3k^3}\partial_\beta g_0|_{\beta=\omega/ck}\right)\\&=ick\omega_p^2F_1\int d\beta\frac{g_0\beta}{(\omega-ck\beta)^2}-\frac{ic^2k^2\omega_p^2F_1}{2\omega}\int d\beta\frac{g_0\beta^2}{(\omega-ck\beta)^2}+\frac{\pi\omega\omega_p^2F_1}{2c^2k^2}\partial_\beta g_0|_{\beta=\omega/ck}.\end{aligned} \tag{20}$$

By expanding the denominator $[1/(\omega-ck\beta)^2]$ up to the square of β, Eq. (20) is reduced to

$$-\frac{ck\omega_p}{\omega}\langle\beta_j^2 e^{-i\phi_j}\rangle=i\frac{1.5\omega_p^2c^2k^2F_1}{\omega^3}\int d\beta g_0\beta^2+\frac{\pi\omega\omega_p^2\partial_\beta g_0}{2c^2k^2}F_1. \tag{21}$$

With a Gaussian distribution $g_0(\beta)=c\sqrt{m/2\pi T}\times\exp(-c^2m\beta^2/2T)$ in Eq. (21) the equation of F_1 in the nontrapping regime becomes

$$\frac{\partial F_1}{\partial t}+i\delta\omega F_1+i\frac{1.5k^2T}{\omega_p m}F_1+\frac{\pi\omega_p^3}{2c^2k^2}[\partial_\beta g_0|_{\beta=\omega/ck}]F_1+K_3=-\frac{ck\omega_p}{4\omega}F_2F_1^*+i\frac{\omega_p}{\omega}\langle P(z_j,t)e^{-i\phi_j}\rangle. \tag{22}$$

We neglected $T\delta\omega/\omega_p$ in Eq. (22). The term involving T in Eq. (22) is the thermal part of the Langmuir wave frequency and the last term is the linear Landau damping coefficient. K_3 is the third-order expansion of the kinetic term, which will be given later.

B. Equation of F_2

The second ($n=2$) kinetic term in the nontrapping regime can be expanded from Eqs. (17) and (19) in the same manner as the $n=1$ case. After some algebra,

$$\begin{aligned}\langle\beta_j^2 e^{-2i\phi_j}\rangle=&-\left(\frac{\omega_p^2}{4\omega^2}+\frac{27c^2k^2\omega_p^2}{8\omega^4}\int g_0\beta^2 d\beta\right)F_1^2-i\frac{3ck\omega_p}{4\omega^2}F_2\int g_0\beta^2 d\beta\\&+\frac{\pi\omega_p\omega^2}{4c^3k^3}[\partial_\beta g_0|_{\beta=\omega/ck}]F_2.\end{aligned} \tag{23}$$

For a Gaussian velocity distribution and from Eqs. (13) and (23), the equation of F_2 in the nontrapping regime becomes

$$\begin{aligned}&\frac{\partial F_2}{\partial t}+i\omega\left(\frac{\omega_p^2}{4\omega^2}-1\right)F_2+i\frac{3k^2\omega_p^2T}{4\omega^3m}F_2-\frac{\pi\omega_p^2\omega}{4c^2k^2}[\partial_\beta g_0|_{\beta=\omega/ck}]F_2+K_4\\&=-\frac{ck\omega_p}{8\omega}\left(1+\frac{2\omega_p^2}{\omega^2}\right)F_1^2-\frac{27ck^3\omega_p^3T}{8m\omega^5}F_1^2-\frac{ck\omega_p}{4\omega}F_3F_1^*,\end{aligned} \tag{24}$$

where K_4 is the fourth-order expansion from the kinetic term (not derived here).

The second harmonic is not directly driven by the external force. Due to $\partial_t F_2\ll\omega F_2$ in the slowly varying limit, a quasisteady state of F_2 is assumed. For the low temperature plasma, the linear Landau damping is negligible. The fourth-order terms, K_4 and $F_1^*F_3$, are not considered in the derivation of the second-order equation. Using $\omega=\omega_p-\delta\omega$ and keeping up to the linear order of T and $\delta\omega$, Eq. (24) becomes

$$\left(1-\frac{8\delta\omega}{3\omega_p}-\frac{k^2T}{m\omega_p^2}\right)F_2=-i\frac{ck}{2(1-2\delta\omega/\omega_p)}\times\left(1-\frac{2\delta\omega}{3\omega_p}+\frac{9k^2T}{m\omega_p^2}\right)F_1^2.$$

Dividing both-hand-sides by $(1-8\delta\omega/3\omega_p-T/\omega_p^2)$ yields

$$F_2 = -i\frac{ck}{2\omega_p}\frac{\left(1-\frac{2\delta\omega}{3\omega_p}+\frac{9k^2T}{m\omega_p^2}\right)}{\left(1-\frac{14\delta\omega}{3\omega_p}-\frac{k^2T}{m\omega_p^2}\right)}F_1^2$$

$$\simeq -i\frac{ck}{2\omega_p}\left(1+\frac{4\delta\omega}{\omega_p}+\frac{10k^2T}{ma_p^2}\right)F_1^2. \quad (25)$$

C. The third-order expansion of the first kinetic term

Here we derive K_3 in Eq. (22), i.e., the third-order expansion of the kinetic term for $n=1$. From this calculation it will be confirmed that there exists no nonrelativistic source of plasma frequency shift at least up to the second order. Instead of pursuing g_3 from the Vlasov equation, which requires a massy algebra, we take the product of separate expansions of β and ϕ in $\langle\beta_j^2 e^{-i\phi_j}\rangle$. To do this we assume a low temperature regime where the thermal velocity is much smaller than the oscillation velocity. When the thermal effect is negligible, the $n=1$ kinetic term is lead by the third order. Thus it is enough to consider only the linear terms of β and ϕ. From the equation of motion,

$$\beta_j = -\frac{iF_1}{2}e^{i\phi_{j0}} + \text{c.c.}, \quad (26)$$

where $\phi_{j0}=kz_{j0}-\omega t$ and z_{j0} the initial position of the jth particle. The position of the jth particle can be written as $z_j=z_{j0}+\zeta_j(z_{j0},t)$. The displacement ζ is, from $c\beta=\dot{\zeta}$,

$$\zeta = \frac{cF_1}{2\omega_p}e^{i\phi_{j0}} + \text{c.c.} \quad (27)$$

From Eqs. (26) and (27), K_3 becomes

$$K_3 = -\frac{ck\omega_p}{\omega}[\langle\beta_j^2 e^{-i\phi_j}\rangle]_{3\text{rd}}$$

$$\simeq \frac{ck\omega_p}{4\omega}\langle(F_1e^{i\phi_{j0}}-\text{c.c.})^2(1-ik\zeta(z_{j0},t))e^{-i\phi_{j0}}\rangle$$

$$= -\frac{ic^2k^2}{8\omega}\langle(F_1^2e^{i\phi_{j0}}-2|F_1|^2e^{-i\phi_{j0}}+F_1^{*2}e^{-3i\phi_{j0}})$$

$$\times(F_1e^{i\phi_{j0}}+F_1^*e^{-i\phi_{j0}})\rangle = \frac{ic^2k^2}{8\omega}|F_1|^2F_1. \quad (28)$$

Note that use was made of $\langle e^{ni\phi_{j0}}\rangle=0$ for $n\neq 0$. Using Eq. (25) with $\delta\omega F_1^2 \ll \delta\omega F_1$ and the thermal effect neglected in the low temperature limit, the third-order term in Eq. (22) can be represented by $ic^2k^2/8\omega|F_1|^2F_1$, which is the same as Eq. (28) and thus cancelled.

In the steady state where the driving and the time derivative terms disappear, Eq. (22) becomes $(\omega_p-\omega+1.5k^2T/\omega_p m)F_1=0$. In the undriven case, ω can be interpreted as the characteristic frequency of the plasma wave.

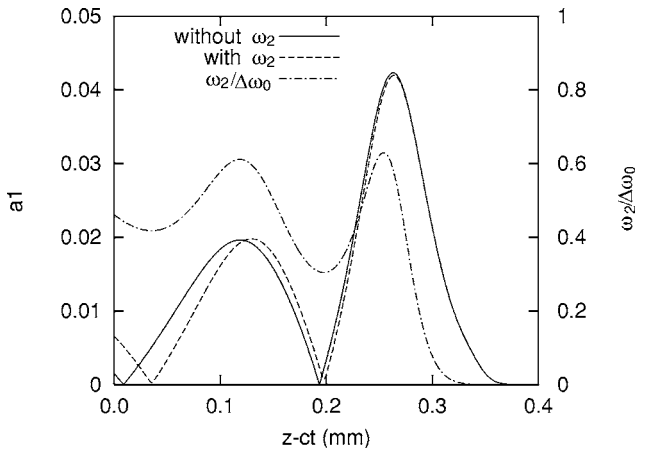

FIG. 1. Numerical solutions of the three-wave model with (solid) and without (dotted) the second-order frequency shift w_2. Here $\Delta\omega_0=1.5k^2T/m\omega_p$ the linear thermal shift of Langmuir wave frequency, and ω_2 is the second-order frequency shift.

Thus the disappearance of every third-order term means that the steady state plasma wave frequency is not modified by the nonlinear harmonics. In the driven case also, this is valid as long as the electric field is dominant over the ponderomotive driving (Raman regime). Then the equation of F_1 in the nontrapping regime takes the following form:

$$\frac{\partial F_1}{\partial t} + i\delta\omega F_1 + i\frac{1.5k^2T}{m\omega_p}F_1 = i\frac{\omega_p}{\omega}\langle P(z_j,t)e^{-i\phi_j}\rangle. \quad (29)$$

Equation (29) is the closed form of the envelope-kinetic equation in the nontrapping regime, which takes the same form as the envelope equation of the plasma wave in the three-wave model.

Note that the cancellation of the third-order terms, K_3 and $F_1^*F_2$ in Eq. (22) is exactly true for cold plasmas. For nonzero temperature, the fluid calculation suggests a second-order frequency shift ω_2 proportional to $|F_1|^2c^2k^4v_t^2/\omega_p^3$, where v_t is the thermal velocity of the plasma. The factor of this term depends on the plasma distribution: for a waterbag model, it is 15/4.[23–25] For a Gaussian distribution, the fluid equation gives approximately 9/8. The second frequency shift is generally small due to its dependence on the amplitude square, but can be comparable to the linear thermal effect $1.5k^2T/\omega_p m$ near the wavebreaking $F_1\sim 1$. In that case, however, ω_2 influences just the peak region of the driving lasers, whose bandwidths are wide enough to cover the additional frequency shift. Furthermore, the wavebreaking occurs with much lower plasma wave amplitude ($F_1<1$) (Ref. 23) for a thermal plasma. Hence, the effect of the second frequency shift is even more reduced. It can be proved from three-wave simulations that the second frequency shift is negligible. Figure 1 shows the numerical solution of the fluid three-wave model,

$$\frac{\partial a_1}{\partial t} + c\frac{\partial a_1}{\partial z} = -\frac{\omega_p}{2}a_2 F_1^*, \quad \frac{\partial a_2}{\partial t} - c\frac{\partial a_2}{\partial z} = \frac{\omega_p}{2}a_1 F_1, \tag{30}$$

and

$$\frac{\partial F_1}{\partial t} + i\delta\omega F_1 + i\left(\frac{1.5k^2T}{m\omega_p} + A\frac{c^2k^4T}{m\omega_p^3}|F_1|^2\right)F_1 = -\frac{c(k_1+k_2)}{4}a_1^* a_2. \tag{31}$$

We used the pump amplitude $a_2=0.008$ and the seed $a_1=0.001$. The results with $A=0$ ($w_2=0$) and $A=2$ are compared in Fig. 1. Though the ratio of ω_2 to the linear Langmuir frequency shift $1.5k^2T/m\omega_p$ reaches up to 0.6, the resultant seed laser profiles show just a minor difference.

IV. TRAPPING EFFECT ON RBS

In this section, we focus on the effects of trapped electrons on Raman backscattering and the laser amplification (Raman backward amplifier, RBA). Three different approaches are taken for the analysis of the kinetic term: kinetic simulations, a heuristic theory, and the test particle method. For self-consistent simulations of the trapping effects, we used the aPIC code,[13] where the plasma is treated fully kinetically and the lasers are calculated from the envelope-kinetic laser equations (1). For comparisons, the fluid three-wave simulations with Eqs. (30) and (31) are also presented. The results of the three-wave model agree excellently with kinetic simulations as long as the pump intensity is low enough to keep the plasma wave under the wavebreaking limit.[11–13] The limit of the pump amplitude to avoid the wavebreaking is roughly $a_2 \sim 0.005$ for $\omega_p/\omega_{\text{laser}} \sim 0.1$. Figure 2 shows the aPIC simulation and the three-wave model for $a_2=0.004$ and $T_e=5$ eV. It is showing the typical behavior of the three-wave model;[8] the seed is initially broadened [Fig. 2(a)] in the linear regime and shortened [Fig. 2(b)] as the pump is depleted. The electron trapping near the peak of the seed is very minor [Fig. 2(c)].

When the pump intensity is high enough to induce severe particle trapping, the fluid and kinetic simulations generate quite different results. Figure 3 represents simulations in such a regime, where we used the pump amplitude $a_2=0.02$ and plasma temperature $T_e=50$ eV. Note that the enhanced pump intensity and plasma temperature (i.e., enhanced over the case of Fig. 2) help efficient particle trapping. The discrepancy between the aPIC simulation and the three-wave calculation is not large in the early stage of the amplification, where trapping is rarely observed. However at $t=1.4$ ps when electrons are severely trapped, the amplification obtained from the aPIC is much lower than that from the three-wave model. The suppression of the amplification is closely related to the broken resonance between the driving (the beat of the lasers) and the plasma wave frequencies. In the nontrapping regime, it was shown that the kinetic term

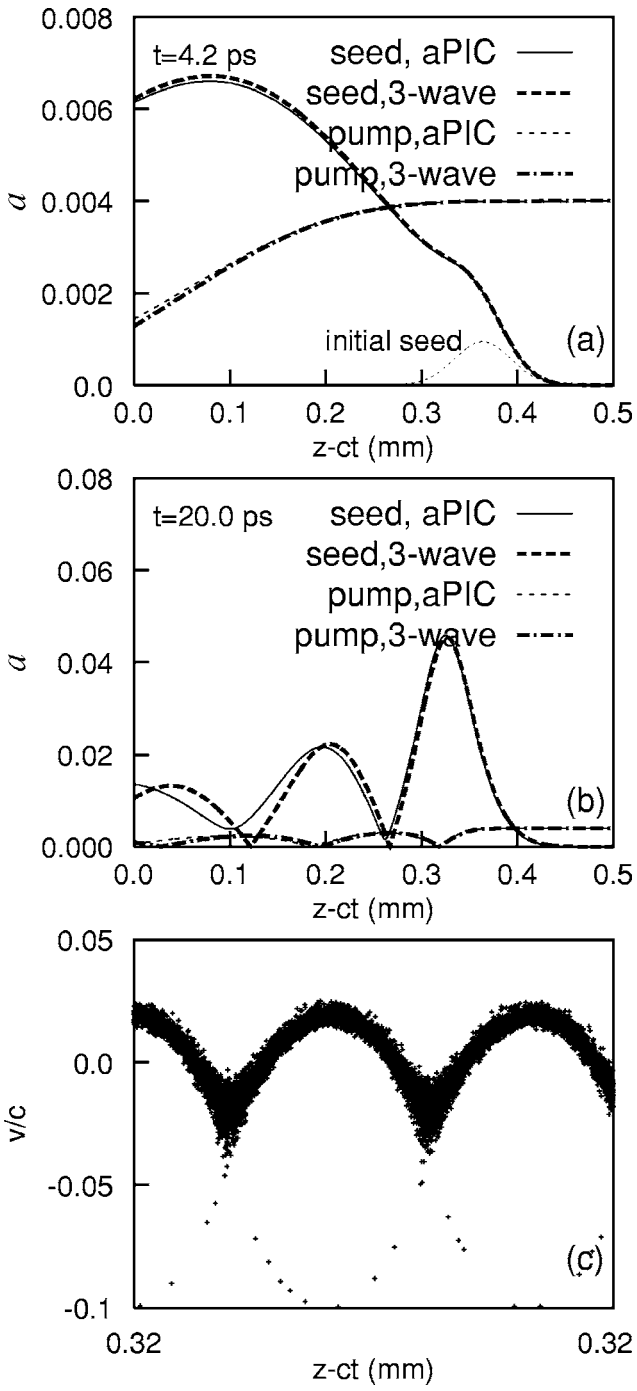

FIG. 2. Laser amplification in the nontrapping regime. The pump amplitude is $a_2=0.004$ and the initial seed amplitude is $a_1=0.000942$. The wavelengths of the seed and pump are $\lambda_1=0.873$ μm and $\lambda_2=0.8$ μm, respectively. The plasma density is $n_e=1.2\times10^{19}$ cm^{-3} and the temperature of the plasma is 5 eV. (a) In the early stage of the amplification, the seed is amplified and broadened. (b) The amplification is in the nonlinear regime (the π-pulse regime). (c) The electron phase space near the peak of the seed in (b).

generated just a thermal shift of the Langmuir frequency. When the electron trapping is significant, the kinetic term generates another frequency downshift via a small fraction of trapped electrons.

To confirm the remark by simulations, a special diagnostic was inserted into the averaged PIC code to monitor $\delta\omega_{\text{trap}}/\omega_p$ during the amplification process. The first har-

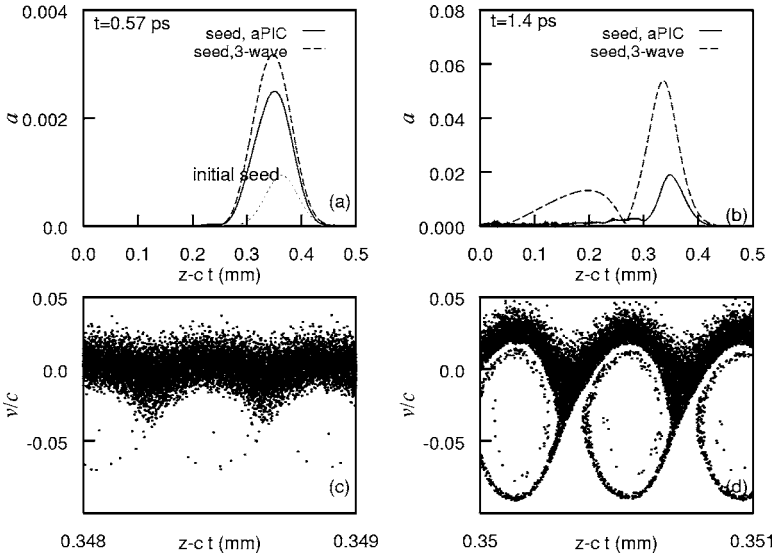

FIG. 3. Laser amplification in the trapping regime. The pump amplitude is $a_2=0.02$. The laser wavelengths and the initial seed amplitude are the same as in Fig. 2. The plasma density and temperature are $n_e=1.05\times10^{19}$ cm^{-3} and 50 eV, respectively. (a), (b) The amplifications at $t=0.57$ ps and 1.4 ps, respectively. (c), (d) Corresponding electron phase spaces near the peaks of the seeds.

monic amplitude F_1 is factored out from the kinetic term as

$$-\frac{ck\omega_p}{\omega}\langle\beta_j^2 e^{-i\phi_j}\rangle = -\frac{ck\omega_p}{\omega|F_1|^2}(F_{1r}\langle\beta_j^2\cos\phi_j\rangle - F_{1i}\langle\beta_j^2\sin\phi_j\rangle)F_1 + i\frac{ck\omega_p}{\omega|F_1|^2}(F_{1i}\langle\beta_j^2\cos\phi_j\rangle + F_{1r}\langle\beta_j^2\sin\phi_j\rangle)F_1, \quad (32)$$

where $F_{1r,i}$ represent the real and imaginary parts of F_1, respectively. The factor of F_1 in the imaginary part of Eq. (32) is the frequency shift $\delta\Omega$, which includes both the thermal and trapping effects ($1.5k^2T/m\omega_p$ and $\delta\omega_{\text{trap}}$, respectively). Then

$$\delta\Omega = \frac{ck\omega_p}{\omega|F_1|^2}(F_{1i}\langle\beta_j^2\cos\phi_j\rangle + F_{1r}\langle\beta_j^2\sin\phi_j\rangle). \quad (33)$$

The real part of Eq. (32) is a damping νF_1, where ν is defined by

$$\nu = -\frac{ck\omega_p}{\omega|F_1|^2}(F_{1r}\langle\beta_j^2\cos\phi_j\rangle - F_{1i}\langle\beta_j^2\sin\phi_j\rangle). \quad (34)$$

Note that the real part is caused by the Landau damping and the energy loss by the plasma wave into the acceleration of the trapped particles. Figure 4 shows $\delta\Omega$ and ν measured from the simulation, where the same parameter set as Fig. 3 was used. In the early stage of the amplification [Fig. 4(a)], where the trapping has not occurred yet, ν is almost zero and $\delta\Omega$ is very close to the thermal correction of the Langmuir frequency as can be expected from the linear analysis in the previous sections. As trapping occurs [Fig. 4(b)], a conspicuous decrease of $\delta\Omega$ is observed with 25% drop at its maximum. The phase spaces at different locations show that the frequency shift has a strong correlation with the particle trapping.

The trapping-induced frequency shift can also be estimated heuristically as follows. The contribution from the trapped particles to the kinetic term can be written as

$$[ck\langle\beta_j^2 e^{-i\phi_j}\rangle]_{\text{trap}} \sim ck\langle\beta_j^2\rangle\langle e^{-i\phi_j}\rangle = i\epsilon\frac{c^2k^2}{2\omega_p}\beta_{\text{trap}}^2 F_1, \quad (35)$$

where β_{trap} is the maximum velocity of the particles trapped and accelerated inside a plasma wave trough and ϵ is the fraction of the trapped particles near the maximum velocity,

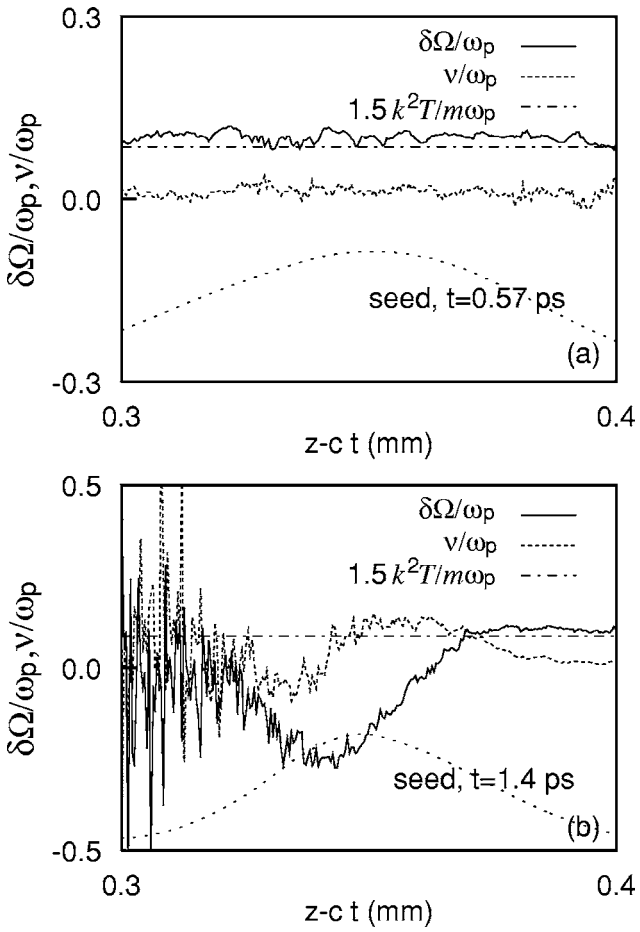

FIG. 4. Measurement of $\delta\Omega$ [Eq. (33)] and ν [Eq. (34)] from the aPIC simulation. The simulation parameters are the same as in Fig. 3.

typically less than 5%. We used Eq. (5) to obtain Eq. (35). From the equation of motion $\dot{\beta} \simeq \omega_p F_1$, the trapped electrons get the energy of $\beta^2 = 4\omega_p F_1 / ck$ in the frame comoving with the phase velocity of the plasma wave ($\beta_\phi = \omega_p / ck$). This corresponds to the maximum velocity in the lab frame

$$\beta_{\text{trap}} \simeq \beta_\phi + 2\sqrt{\frac{\omega_p}{ck} F_1}. \tag{36}$$

Equation (35) can be set as $i\delta\omega_{\text{trap}} F_1$, where $\delta\omega_{\text{trap}}$ is the frequency shift by the trapped particles. From Eqs. (35) and (36),

$$\frac{\delta\omega_{\text{trap}}}{\omega_p} \simeq \frac{\epsilon}{2}\left(1 + 4\sqrt{\frac{F_1}{\beta_\phi}} + \frac{4F_1}{\beta_\phi}\right). \tag{37}$$

The trapping occurs near the wavebreaking limit, where the amplitude of the electron velocity is larger than the phase velocity of the plasma wave. Thus the phase velocity in Eq. (37) can be approximated as $\beta_\phi \lesssim \beta \simeq F_1$. From an empirical parameter $\epsilon \sim 0.05$ along with this approximation, the frequency shift by the trapped particles are found to be about 20% of the plasma frequency ($\delta\omega_{\text{trap}} / \omega_p \sim 0.2$), which is consistent with the simulation in Fig. 4.

In the previous analysis of the trapping effects,[7] the envelope-kinetic model for the plasma wave was established but it was not fully closed. In Sec. III, the closure in the nontrapping regime was presented from the linear analysis of the kinetic term. We found that the conventional three-wave fluid model is exact up to the third order in this regime. Analytic theory which predicts the fraction ϵ and other factors in Eq. (37) more exactly is expected to be published soon.[25] In this paper, we suggest the test particle method to numerically close Eq. (12). In this scheme, we assume that the kinetic term can be split into the thermal frequency shift, third-order contribution, and the trapping terms. The first two terms were investigated in Sec. III, which are assumed to be scarcely modified by the trapped particles because the fraction of the trapped particles is very small and main bulk of the plasma remains untrapped. Then Eq. (12) can be rewritten as

$$\frac{\partial F_1}{\partial t} + i\left(\delta\omega + \frac{1.5k^2T}{m\omega_p}\right)F_1 + K_t = -\frac{c(k_1 + k_2)}{4} a_1^* a_2, \tag{38}$$

where the trapping portion of the kinetic term K_t is defined by

$$K_t = -\frac{ck\sum_{\text{trapped}} \beta_j^2 e^{-i\phi_j}}{N}. \tag{39}$$

In Eq. (39), N is the total number of particles in λ_b. The summation goes over the trapped particles only. Note that in Eq. (38) the third-order contribution from the kinetic term was used to cancel out $ck\omega_p F_2 F_1^* / 4\omega$ in Eq. (12) and the general driving force $P(z_j, t)$ was replaced by the ponderomotive force of the two counterpropagating lasers. Now let us describe the outline of the test particle scheme as follows. The equations to be solved are Eqs. (30) and (38), which are the same as the three-wave fluid equations except the trapping term K_t. To include K_t self-consistently in the numerical solution of Eq. (38), we employ a small number of test particles (electrons), which follow the equation of motion but do not generate any electric field. Every time step the trapping term K_t is calculated from the test particles, and the renewed value of K_t is used again to upgrade the electric field by solving Eq. (38). Then the test particles are pushed to the next time step by the new electric field and the ponderomotive force of the lasers.

Though the lasers are driven only by the first harmonic F_1, the particles follow the full harmonics of the electric field. The effects of higher harmonics can be important in the sense that the trapping can be enhanced by the sharp nodes generated by the high frequency components and also the particle acceleration inside the plasma wave should be different from a single harmonic case. In our simulations, the electric field is pursued up to the third order

$$\frac{eE}{mc\omega_p} = \frac{1}{2}(F_1 e^{i\phi} + F_2 e^{2i\phi} + F_3 e^{3i\phi}) + \text{c.c.}, \tag{40}$$

where F_1 and F_2 are calculated from Eqs. (25) and (38), respectively, and F_3 is determined by $F_3 = -3c^2k^2F_1^3 / 8\omega_p^2$. The third harmonic F_3 was obtained from the simple expansion of the fluid equations.

The test particle scheme is numerically advantageous, because the number of simulation particles can be much smaller than in the full kinetic aPIC simulations. This is possible due to the fact that only the electrons in the tail of the Gaussian velocity distribution are relevant to the trapping. We do not need to load the whole N particles in a beat wavelength, but have only to follow a much smaller number of particles located in the high velocity region. In the simulations presented in this paper, we loaded particles whose velocities are between -0.5σ and -3.0σ for the Gaussian velocity distribution $\exp(-v^2/\sigma^2)$. In this case the number of test particles per a beat wavelength corresponds to $0.25N$. Note that the absence of the Poisson solver make the test particle simulation even faster. Typical gain in the computation speed over the aPIC simulation was about 10.

Some benchmarkings of the test particle scheme were made against the full aPIC and fluid simulations. Figure 5 shows the comparison of the aPIC, test particle, and three-wave simulations for a strong pump case $a_2 = 0.02$. The test particle simulation reproduces well the leading peak of the amplified seed laser. In the tail part of the seed, the aPIC simulation shows that the plasma wave is destroyed completely by the wavebreaking and the interaction between the three-waves stops. In the test particle model, however, such a wave breaking cannot be properly described, which is thought to be the source of the discrepancy in the tail. Figure 6 represents a similar simulation with a weaker pump laser ($a_2 = 0.01$). The trapping is still dominant and the aPIC results are much lower than the fluid calculation. The test particle simulation shows a good agreement with the aPIC results.

V. SUMMARY

The electron kinetic effects on the RBS were studied in the framework of the envelope-kinetic model of a plasma

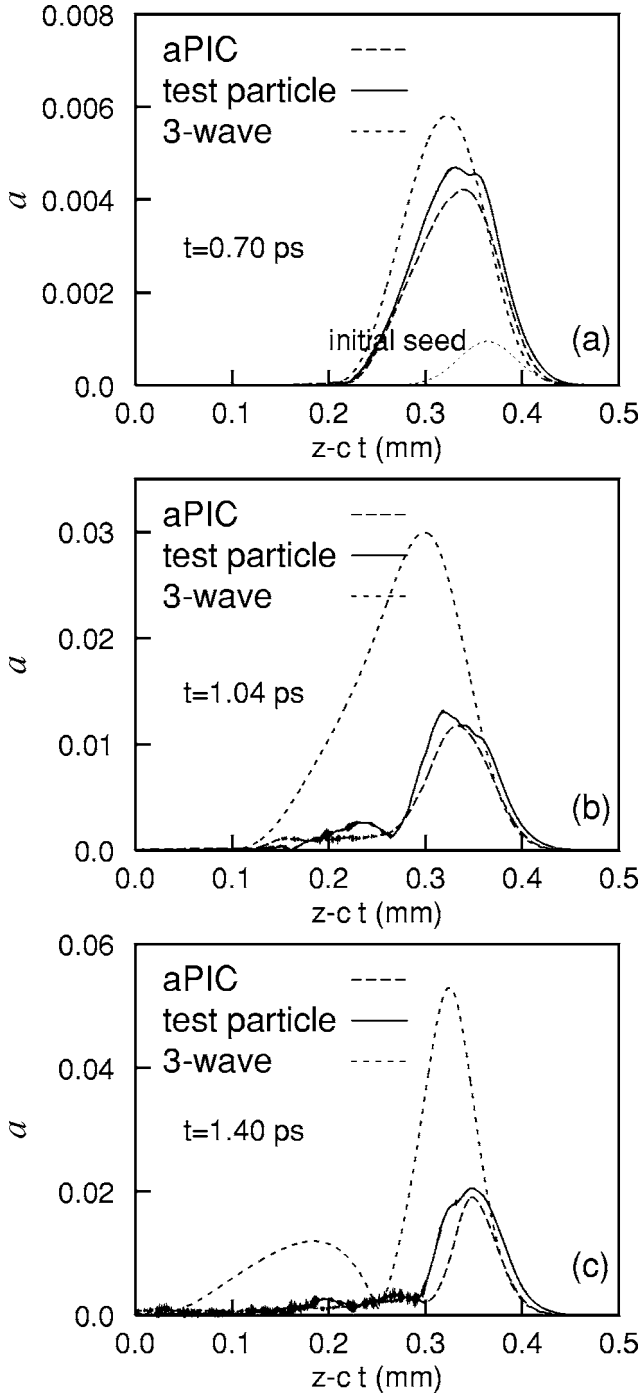

FIG. 5. Simulations of the strong pump case (parameters are the same as in Fig. 3) using aPIC, test particle scheme, and the three-wave fluid model.

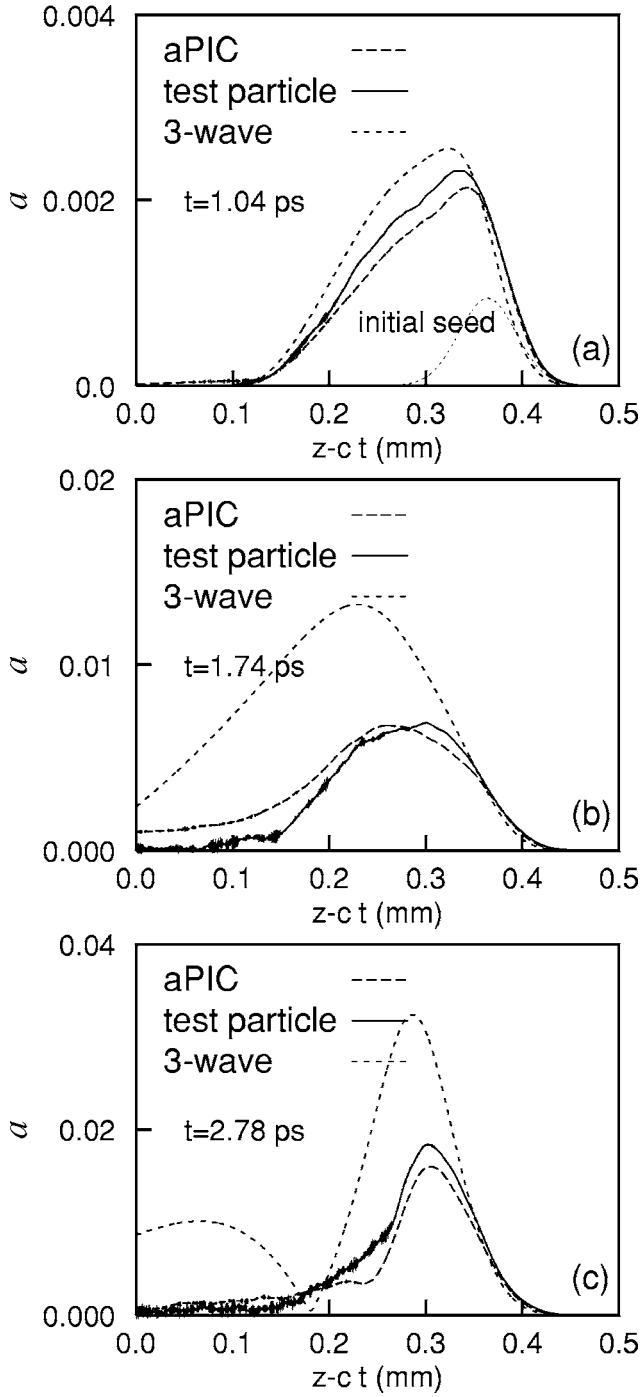

FIG. 6. Comparisons of the three different schemes. Parameters are the same as in Fig. 5, except the pump amplitude $a_2=0.01$.

wave. The envelope-kinetic equations were derived for general harmonics of the plasma wave. The equation for the first harmonic envelope F_1 takes a form similar to what is used in the three-wave fluid model but a kinetic term is introduced. One major goal of this paper was to close the envelope-kinetic equation of the plasma wave, which was not covered in the previous work.[7] To close the envelope-kinetic equation, we analyzed the kinetic term in the nontrapping and trapping cases in the low temperature regime. When the pump laser amplitude is small (typically $a_2<0.005$ for $\omega_p/\omega\sim0.1$), the electron trapping is negligible (nontrapping regime), and the kinetic term generates the thermal shift of the Langmuir wave frequency. The resulting closed equation is the same as that used in the three-wave fluid model. This implies that the three-wave model for RBS is exact at least up to the third order. In the regime of severe electron trapping (but the fraction is still small, typically less than 5%) which is caused by a large pump intensity and a high temperature of the plasma, the trapped electrons shift down the plasma wave frequency considerably (it was 20% of the plasma frequency for $a_2=0.02$). The resonance breaking by this shift significantly suppresses RBS and the laser amplifi-

cation. The envelope-kinetic model in the trapping regime could be closed by the test particle method. We obtained a good agreement between the simulations from the full kinetic (aPIC) and test particle codes.

ACKNOWLEDGMENTS

We thank R. Lindberg, A. Charman, and J. Wurtele of UC Berkeley/LBNL for constructive discussions. We also appreciate the helpful comments by G. Shvets.

This work was financially supported by the Creative Research Initiatives program/KOSEF of the Korea Ministry of Science and Technology.

[1] B. J. MacGowan, B. B. Afeyan, C. A. Back, R. L. Berger, G. Bonnaud, M. Casanova, B. I. Cohen, D. E. Desenne, D. F. DuBois, A. G. Dulieu, K. G. Estabrook, J. C. Fernandez, S. H. Glenzer, D. E. Hinkel, T. B. Kaiser, D. H. Kalantar, R. L. Kauffman, J. D. Moody, D. H. Munro, L. V. Powers, H. A. Rose, C. Rousseaux, R. E. Turner, B. H. Wilde, S. C. Wilks, and E. A. Williams, Phys. Plasmas **3**, 2029 (1996).
[2] R. E. Giacone and H. X. Vu, Phys. Plasmas **5**, 1455 (1998).
[3] D. A. Russell, D. F. DuBois, and H. A. Rose, Phys. Plasmas **6**, 1294 (1999).
[4] J. C. Fernández, J. A. Cobble, D. S. Montgomery, M. D. Wilke, and B. B. Afeyan, Phys. Plasmas **7**, 3743 (2000).
[5] H. X. Vu, D. F. DuBois, and B. Bezzerides, Phys. Rev. Lett. **86**, 4306 (2001); Phys. Plasmas **9**, 1745 (2002).
[6] S. Brunner and E. J. Valeo, Phys. Rev. Lett. **93**, 145003 (2004).
[7] M. S. Hur, R. R. Lindberg, A. E. Charman, J. S. Wurtele, and H. Suk, Phys. Rev. Lett. **95**, 115003 (2005).
[8] V. M. Malkin, G. Shvets, and N. J. Fisch, Phys. Rev. Lett. **82**, 4448 (1999); Phys. Plasmas **7**, 2232 (2000); Phys. Rev. Lett. **84**, 1208 (2000).
[9] D. Strickland and G. Mourou, Opt. Commun. **56**, 219 (1985).
[10] G.-Z. Sun, E. Ott, Y. C. Lee, and P. Guzdar, Phys. Fluids **30**, 526 (1987).
[11] D. S. Clark and N. J. Fisch, Phys. Plasmas **10**, 3363 (2003); **10**, 4848 (2003).
[12] M. S. Hur, I. Hwang, and H. Suk, J. Korean Phys. Soc. **47**, 625 (2005).
[13] M. S. Hur, G. Penn, J. S. Wurtele, and R. R. Lindberg, Phys. Plasmas **11**, 5204 (2004).
[14] A. A. Balakin, D. V. Kartashov, A. M. Kiselev, S. A. Skobelev, A. N. Stepanov, and G. M. Fraiman, JETP Lett. **80**, 12 (2004).
[15] Y. Ping, W. Cheng, S. Suckewer, D. S. Clark, and N. J. Fisch, Phys. Rev. Lett. **92**, 175007 (2004).
[16] W. Cheng, Y. Avitzour, Y. Ping, S. Suckewer, N. J. Fisch, M. S. Hur, and J. S. Wurtele, Phys. Rev. Lett. **94**, 045003 (2005).
[17] G. Shvets, J. S. Wurtele, and B. A. Shadwick, Phys. Plasmas **4**, 1872 (1997).
[18] G. Shvets, N. J. Fisch, A. Pukhov, and J. Meyer-ter-Vehn, Phys. Rev. Lett. **81**, 4879 (1998).
[19] R. J. Noble, Phys. Rev. A **32**, 460 (1985).
[20] J. T. Mendonça, J. Plasma Phys. **34**, 115 (1985).
[21] C. J. McKinstrie and D. W. Forslund, Phys. Fluids **30**, 904 (1987).
[22] W. B. Mori, IEEE Trans. Plasma Sci. **15**, 88 (1987).
[23] T. P. Coffey, Phys. Fluids **14**, 1402 (1971).
[24] R. L. Dewar and J. Lindl, Phys. Fluids **15**, 820 (1972).
[25] R. R. Lindberg, A. E. Charman, M. S. Hur, and J. S. Wurtele, Bull. Am. Phys. Soc. 47th Annual DPP Meeting, 219 (2005).